

Influence of the Shape of the Beampipe on the Luminosity Measurement at the ILC

LC-PHSM-2008-007

H. Abramowicz, R. Ingbir, S. Kananov, A. Levy, I. Sadeh

School of Physics and Astronomy, The Raymond and Beverly Sackler Faculty of Exact Sciences, Tel Aviv University, Tel Aviv, Israel.

October 2008

Abstract

Measurement of the luminosity at the International Linear Collider will be accomplished by counting the number of Bhabha scattering events at small angles. This measurement depends on the amount of material which is placed in front of the luminosity calorimeter, due to possible pre-showering of particles. In the current detector layout no such material is foreseen, owing to the structure of the beampipe. Here, an alternative design is considered, for which particles pass through the beampipe before reaching the luminosity calorimeter. The subsequent effect on the luminosity measurement is studied.

1 Introduction

In this study the influence of the shape of the beampipe on the luminosity measurement at the International Linear Collider (ILC) is studied. Luminosity is measured at the ILC by counting the number of Bhabha scattering events at low angles [1]. This is accomplished by a dedicated calorimeter, LumiCal.

In the current detector layout [2, 3], LumiCal is placed 2.27 m from the interaction point (IP). LumiCal is a tungsten-silicon sandwich calorimeter. The inner radius of LumiCal is 80 mm, and its outer radius is 190 mm, resulting in a polar angular coverage of 35 to 84 mrad.

In the current detector layout the beampipe, which is made of Beryllium, has a so called *conical* shape. The inner radius close to the IP ($Z = 0$) is small, so as to accommodate the vertex detector. At larger distances from the IP, up to the first layer of LumiCal ($Z = 2.27$ m), the radius increases, as illustrated in Fig. 1.

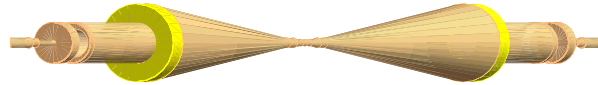


Figure 1: Schematic design of the conical shape of the beampipe in the current detector design. The color of the beampipe is brown, and that of LumiCal is yellow.

This design has the benefit that particles which enter LumiCal do not pass through any material beforehand¹. On the other hand, this configuration has several deficiencies. For one, it is difficult to maintain the vacuum inside the beampipe around the edges of LumiCal, where the radius of

¹ Here the vertical beampipe wall, which is placed in front of LumiCal, need not be taken into account. Any pre-showering which occurs there does not affect the development of showers in LumiCal, since the distance between the beampipe wall and LumiCal is insignificant

the beampipe is large. Another difficulty lies in power-loss as a result of high order electromagnetic (EM) modes [4]. In addition, the conical shape of the beampipe may cause disturbances of the magnetic field around LumiCal.

In order to prevent these problems an alternative, so called *parallel*, shape of the beampipe is proposed. In this case the Beryllium beampipe has uniform inner and outer radii of 5.5 and 6 cm respectively. These dimensions were chosen, so as to minimize the thickness of the beampipe, while clearing enough space for the beams in the 14 mrad crossing-angle scenario. The design of the parallel shape is illustrated in Fig. 2.



Figure 2: Schematic design of the proposed parallel shape of the beampipe. The color of the beampipe is brown, and that of LumiCal is yellow.

In the parallel configuration, for the angular range of LumiCal, $35 < \theta < 84$ mrad, particles pass through Beryllium of thickness between 5.9 and 14.3 cm. This corresponds to between 0.17 and 0.41 of the radiation length, between 0.15 and 0.35 of the nuclear interaction length and between 0.2 and 0.47 of the nuclear collision length in Beryllium [5]. The downside of the parallel configuration is, therefore, the fact that particles which enter LumiCal may pre-shower, as a result of the passage through the material of the beampipe.

Since particles which enter LumiCal traverse the beampipe at $Z > 65$ cm, the structure of the beampipe near the IP does not affect the luminosity measurement. One may, therefore, choose a different design at low Z in order to clear space for the vertex detector. The current configuration was chosen for its simplicity.

2 Luminosity Measurement

The measured luminosity is defined as

$$\mathcal{L} = \frac{N_{\text{Bh}}}{\sigma_{\text{Bh}}}, \quad (1)$$

where N_{Bh} is the counted number of Bhabha events in a well-defined polar angular range and σ_{Bh} is the integrated Bhabha cross-section in this range. The requirement for LumiCal is to enable a measurement of the integrated luminosity with a relative precision of about 10^{-4} [6, 2].

A set of topological cuts is applied in order to distinguish Bhabha scattering from the background processes. This is done by comparing the position and the energy of EM showers, which are initiated in the two arms of LumiCal by the scattered particles. The amount of energy in each arm relative to the beam energy is also constrained, and the reconstructed position of each shower must lie within the fiducial volume (acceptance region) of the detector [7, 8, 9] (see Sect. 4 below).

Several factors, such as the energy resolution and the bias in the reconstruction of the position of showers, induce an error in the luminosity measurement [2, 3]. The error manifests as miss-counting of the number of expected Bhabha scattering events within the fiducial volume. It is convenient to define the relative bias in counting as

$$\delta\mathcal{N} \equiv \frac{N_{\text{gen}} - N_{\text{rec}}}{N_{\text{gen}}} \Bigg|_{\theta_{\text{min}}^f}^{\theta_{\text{max}}^f}, \quad (2)$$

where N_{rec} and N_{gen} are respectively the number of reconstructed and generated Bhabha events, and θ_{min}^f and θ_{max}^f are the respective low and high bounds on the fiducial volume of LumiCal. Accordingly, the relative error of the integrated luminosity, \mathcal{L} , comes down to

$$\frac{\Delta\mathcal{L}}{\mathcal{L}} = \delta\mathcal{N}. \quad (3)$$

3 Physics Sample

The physics sample which was investigated consisted of 10^6 Bhabha scattering events with center-of-mass energy $\sqrt{s} = 500$ GeV. The events were generated using BHWIDE, version 1.04 [10]. BHWIDE is a wide angle Bhabha MC, which contains

the electroweak contributions, which are important for the high energy e^+e^- interactions considered here. The sample contains only events in which the leptons are scattered within $35 < \theta < 84$ mrad, which is the physical polar angular range of LumiCal.

The response of LumiCal to the passage of particles was simulated using MOKKA, version 06-05-p02 [11]. MOKKA is an application of a general purpose detector simulation package, GEANT4, of which version 9.0.p01 was used [12]. The GEANT4 range-cut parameter was set to 0.005 mm. The MOKKA model which was used is LDC00_03Rp, where several of the internal structure parameters of LumiCal were altered [2]^{II}.

Strictly speaking, Born-level elastic Bhabha scattering does not occur. In practice, the process is accompanied by the emission of electromagnetic radiation, $e^+e^- \rightarrow e^+e^-\gamma$. Figure 3 shows the polar production angle of scattered leptons and radiative photons. Each distribution is normalized independently of the other. The distribution of the polar angle is cut according to the fiducial volume of LumiCal. The fiducial volume of LumiCal is defined by $\theta_{min}^f = 0.41$ mrad and $\theta_{max}^f = 0.69$ mrad. This angular range is smaller than the full angular coverage of LumiCal, as only EM showers which are fully contained in LumiCal are reconstructed [3].

4 Bhabha Event Reconstruction

Each particle that enters LumiCal initiates an EM shower. Due to the fact that both leptons and photons enter LumiCal, the separate showers inter-mix to various degrees, depending on the initial angular separation between the particles. The typical signature of Bhabha scattering events is therefore the presence of several showers, back to back in the detector.

Since LumiCal has a finite spatial resolution, the first step in the Bhabha selection process is the clustering of showers in each arm of the detector. It has been shown [14] that for the current design of Lumi-

^{II} This set of parameters was chosen following internal discussions within the FCAL collaboration [13].

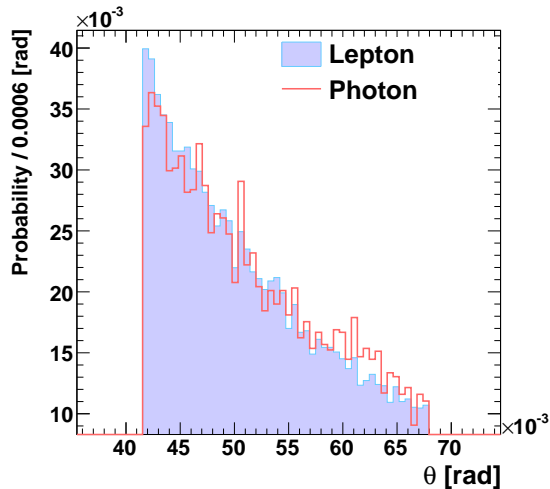


Figure 3: Normalized distributions of the production polar angle, θ , of leptons and of photons, as denoted in the figure.

Cal, it is possible to separate a pair of showers using a dedicated clustering algorithm, provided that

$$d_{pair} \geq R_M \quad \text{and} \quad E_{sh} \geq 20 \text{ GeV}, \quad (4)$$

where d_{pair} is the distance between the centers of the two showers, R_M is the Molière radius of LumiCal^{III} and E_{sh} is the energy of each of the showers.

In the present design of LumiCal there is no way to distinguish between EM showers initiated by leptons and those started by photons. One may, therefore, consider instead the cluster which has the highest energy in each arm, and impose on it the Bhabha selection cuts. Only clusters which are fully contained within LumiCal are considered. The set of selection cuts used in the following study are [8]

^{III} The Molière radius is the distance around the center of an EM shower, in which, on average, 90% of the energy of the shower may be found. For the current design of LumiCal $R_M = 14$ mm.

$$\frac{|E_r - E_l|}{\min\{E_r, E_l\}} \leq 10\% \quad , \quad E_r, E_l \geq E_{beam} \cdot 80\% \quad ,$$

$$|\theta_r - \theta_l| \leq 1 \text{ mrad} \quad \text{and} \quad \theta_{min}^f \leq \theta_r, \theta_l \leq \theta_{max}^f \quad (5)$$

where E_r and E_l (θ_r and θ_l) are, respectively, the energy (polar angle) of the highest-energy cluster in the right and left arms of LumiCal. The symbol E_{beam} refers to the beam energy.

5 Pre-Showering in the Material of the Beampipe

Figure 4 shows the correlation between the position relative to the IP of the creation of particles, Z_0 , and the energy of the created particle. Both the conical and the parallel configurations were simulated, using 10^4 Bhabha events. For the conical configuration no particles are created between the IP ($Z = 0$) and the first plane of LumiCal ($Z = 2.27$ m), while for the parallel design, this is not the case. The rate of particle creation as a function of the distance from the IP is in accordance with the polar angular dependence of the Bhabha scattering cross section (see Fig. 3).

We shall refer to particles which were generated according to the Bhabha cross section at the IP, as *primary particles*. Particles which were created in the simulation due to pre-showering in the material of the beampipe ($Z_0 > 0$) will be referred to as *secondary particles*. A *primary parent* of a given secondary particle is defined as the primary particle, that initiated the shower, in which the secondary was created.

6 Comparison Between the Two Designs

In order to estimate the effect on the luminosity measurement of changing the shape of the beampipe, it is necessary to know the change in the counting rate of Bhabha events between the two designs. We assume for this purpose that in the conical configuration all of the systematic errors

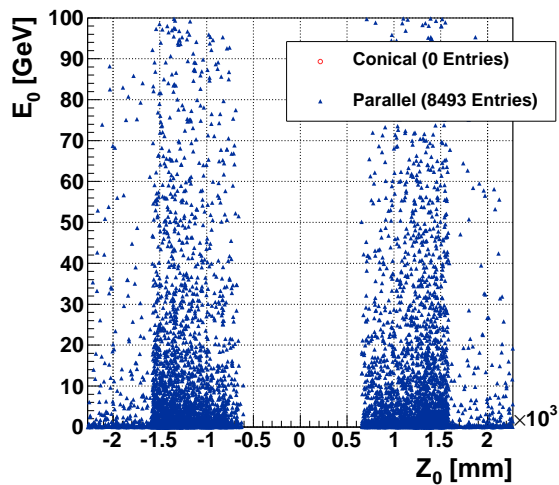


Figure 4: Correlation between the position relative to the IP of the creation of particles, Z_0 , and the energy of the created particle, E_0 . Both the conical and the parallel configurations were simulated, as indicated in the figure, using 10^4 Bhabha events.

are accounted for. Any miss-counting will therefore be due to pre-showering within the material of the beampipe, which instigates additional EM showers in LumiCal.

The relative bias in the measurement would now be given by Eqs. (2) and (3), with the substitutions

$$N_{gen} \rightarrow N_{con} \quad \text{and} \quad N_{rec} \rightarrow N_{par}, \quad (6)$$

where N_{con} and N_{par} are, respectively, the number of Bhabha events in the conical and parallel configurations which pass the Bhabha selection cuts (see Sect. 4). By making this estimation of $\Delta\mathcal{L}/\mathcal{L}$, we observe directly the difference in the counting rate of Bhabha events between the two beampipe configurations. Both the “generated” N_{con} and the “reconstructed” N_{par} are calculated after the initial sample of events goes through clustering and passes the selection cuts. This way all of the other systematic effects are canceled and we are left with just the error which is associated with the change in geometry.

It is helpful to begin by performing a case-by-case comparison of the two configurations. For

any given event, either the two designs yield the same result (success or failure of the cuts), or in one configuration the event passes the cuts while in the other it does not. Possible differences between the two designs for a hypothetical sample of five Bhabha events are given in Table 1.

Event index	Success/failure of selection cuts	
	Conical	Parallel
1	✓	✓
2	×	×
3	✓	×
4	×	✓
5	✓	×

Table 1: Success (✓) or failure (×) of the Bhabha selection cuts for the conical and parallel designs, using a hypothetical sample of five Bhabha events.

We define the *selection efficiency* as the percentage of events which passed the selection cuts out of the entire sample of events. In this example, therefore, the selection efficiency is 60% for the conical design, and 40% for the parallel design. Subsequently, the relative bias in luminosity (in the counting rates) between the two configurations is

$$\delta\mathcal{N} = \frac{N_{con} - N_{par}}{N_{con}} = \frac{3 - 2}{3} = 33\%. \quad (7)$$

It should be noticed that despite the fact that there is a miss-match between the two configurations in three cases out of five, two of the miss-matches cancel each other out, and the final difference is one case out of five. This example reflects the results which were obtained for the real event sample.

We now move on to the physics sample of 10^6 Bhabha scattering events which was generated using BHWIDE. The entire sample was divided into groups of 10^3 events. For each event, clustering was performed in each arm, and the clusters were subjected to the selection cuts.

It is convenient to define the variable $N_{par}^{(\checkmark)}$,

which counts the number of events out of a single group of 10^3 events, in which the Bhabha selection cuts passed in the parallel configuration, but not in the conical. Similarly, $N_{par}^{(\times)}$ counts the number of individual failures of the selection cuts in the parallel configuration.

Figure 5 shows the correlation between $N_{par}^{(\checkmark)}$ and $N_{par}^{(\times)}$ for the entire sample of 10^3 groups of 10^3 events. For many of the event groups $N_{par}^{(\checkmark)} = N_{par}^{(\times)}$. This means that even though there are miss-matches in the selection efficiency on a case-by-case basis, the total efficiency for the entire group of 10^3 events is the same for both configurations. For bins with $N_{par}^{(\checkmark)} \neq N_{par}^{(\times)}$ there is an accumulated miss-match. This produces a bias in the selection efficiency, since the total number of events which passed the cuts in the two configurations is not the same.

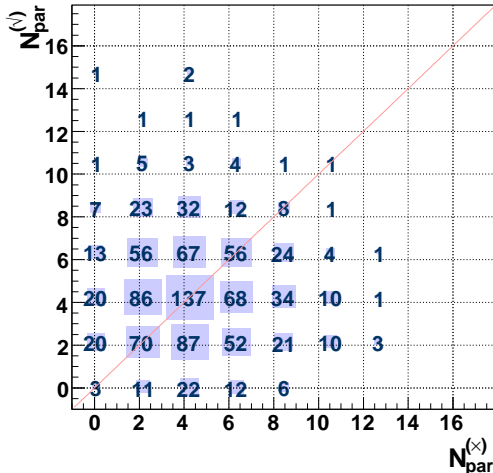


Figure 5: Correlation between the number of individual success, $N_{par}^{(\checkmark)}$, and the number of individual failures, $N_{par}^{(\times)}$, of the Bhabha selection cuts in the parallel configuration, out of groups of 10^3 Bhabha events. In total 10^3 such event groups were considered.

In Fig. 6 is shown the distribution of the relative bias in the Bhabha counting rate, $\delta\mathcal{N}$, for each event group. The values of the mean and of the root-mean-square of the distribution are $(1 \pm 2) \cdot 10^{-4}$

and $(6.6 \pm 0.2) \cdot 10^{-3}$ respectively^{IV}.

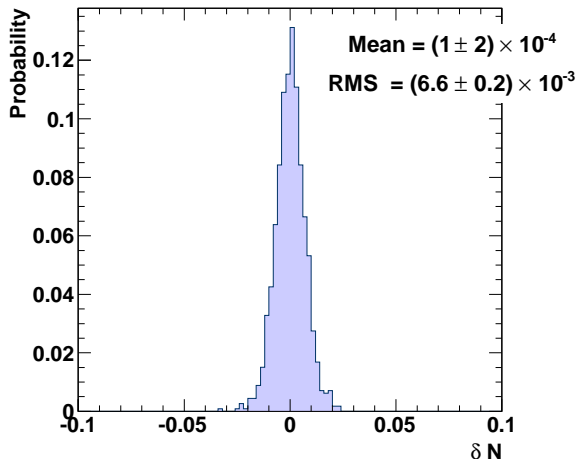


Figure 6: Distribution of the relative bias in the Bhabha counting rate, $\delta N = (N_{con} - N_{par})/N_{con}$, as a result of the change in the design of the beampipe. Each entry represents the value of δN for a group of 10^3 Bhabha events.

7 Conclusions

The small bias in the counting rates (Fig. 6) is accounted for by the fact that for large data samples, the event-by-event differences in the selection efficiency tend to cancel out. As explained above, the difference between the two configurations is the addition of secondary particles, which are created due to passage of the primary particles through the beampipe. The fact that clustering is employed serves to lessen the divergences of the parallel configuration from the conical. This is due to the fact that most of the secondary particles are of low energy, and enter LumiCal in close proximity to their respective primary parents. As such, the showers of the secondary particles are clustered into those of their primary parents.

The main effect, therefore, comes down to a small change in the reconstructed position of clusters, relative to the respective clusters, which would

^{IV} The errors on the fit results are determined by statistics, and may be reduced by considering a larger data sample.

have been reconstructed in the conical configuration. The secondary particles either increase or decrease the reconstructed polar angle of the highest energy clusters with equal probability. This effect, therefore, sometimes serves to increase and sometimes to decrease the value of $|\theta_r - \theta_l|$. Clusters are also pushed into or out of the fiducial volume of LumiCal in the same rate.

The symmetric change of polar angle is due to single scattering of particles. Contrarily, double scattering, in which two photons are emitted in one Compton scattering process, can cause an asymmetric bias in the polar angle. While the present study indicates that this effect is negligible at the level of precision which is needed for the luminosity measurement. A dedicated study should be performed in order to confirm this conjecture.

Differences in the energy of clusters between the two configurations may also occur, for instance, when a shower initiated by a secondary particle is clustered along with a shower which was not a product of the respective primary parent. Another factor that should be considered is the loss or gain of energy in each arm of LumiCal. This may happen when a particle enters the fiducial volume of LumiCal in one configuration, but not in the other. Since the selection cut on energy is loose relative to the polar cut, these effects are less significant than the changes in polar angle.

8 Summary

In order to resolve problems relating to the magnetic field and to the vacuum system, an alternative design of the beampipe has been suggested. In the new configuration, particles which enter the luminosity calorimeter traverse the material of the beampipe beforehand. As a result secondary particles are created due to pre-showering.

The amount and characteristics of pre-showering is determined by the thickness and composition of the beampipe. It has been shown that, for the proposed design, this effect induces a relative bias of $\mathcal{O}(10^{-4})$ in the efficiency of the Bhabha selection process. This, in turn, can produce a relative bias of the same order in the luminosity measurement, if the effect is not accounted for.

The conclusion, therefore, is that for the beampipe design which has been proposed here, the error in the luminosity measurement due to the bias can be controlled. In order to accomplish this, the study which was described here would have to be repeated with a much larger data sample. In this way the error on the fit of the mean value of δN may be reduced to an acceptable level. The effect of double scattering within the beampipe should be studied in detail as well, in order to confirm that the subsequent polar bias is controllable. Further study is also needed in order to determine the dependence of the bias on the choice of Bhabha selection cuts and on the effectiveness of the clustering procedure.

It must be emphasized that for a thicker beampipe, or for a beampipe which is made of material which is heavier than beryllium, the bias due to pre-showering will increase. The shape of the beampipe which will finally be chosen, will have to be known and simulated precisely in order to control this effect.

Acknowledgments

This work is partly supported by the Commission of the European Communities under the 6th Framework Programme “Structuring the European Research Area”, contract number RII3-026126, and by the Israeli Science Foundation. We would like to thank Wolfgang Lohmann for his helpful comments and suggestions.

References

- [1] M. Caffo *et al.*, “Bhabha Scattering,” *Z Physics at LEP1*, *CERN Report 89-08*, 1, 1989. URL: http://documents.cern.ch/cgi-bin/setlink?base=cernrep&categ=Yellow_Report&id=89-08_v1.
- [2] I. Sadeh, “Luminosity Measurement at the International Linear Collider.” URL: http://alzt.tau.ac.il/~sadeh/mscThesis/iftachSadeh_mscThesis.pdf, 2008.
- [3] H. Abramowicz *et al.*, “Redefinition of the Geometry of the Luminosity Calorimeter,” *EUDET-Memo-2008-09*, 2008. URL: <http://www.eudet.org>.
- [4] H. Yamamoto, “Heating of IR region.” Talk given at the 2007 ILC Interaction Region Engineering Design Workshop. URL: <http://www-conf.slac.stanford.edu/ireng07/default.htm>.
- [5] W.-M. t. Yao, “Review of Particle Physics,” *Journal of Physics G 33*, 2006. URL: <http://pdg.lbl.gov>.
- [6] K. Mönig, “Physics Needs for the Forward Region.” Talk given at the Zeuthen FCAL meeting, Aug. 2004.
- [7] A. Stahl, “Luminosity Measurement via Bhabha Scattering: Precision Requirements for the Luminosity Calorimeter,” *LC-DET-2005-004*, 2005. URL: <http://www-flc.desy.de/lcnotes/notes/LC-DET-2005-004.ps.gz>.
- [8] R. Ingbir, “A Luminosity Detector for the International Linear Collider.” URL: <http://alzt.tau.ac.il/~ronen/>, 2006.
- [9] H. Abramowicz *et al.*, “A Luminosity Detector for the International Linear Collider,” *LC-DET-2007-006*, 2007. URL: <http://www-flc.desy.de/lcnotes/notes/LC-DET-2007-006.pdf>.
- [10] S. Jadach, W. Placzek, and B. F. L. Ward, “BHWIDE 1.00: O(alpha) YFS exponentiated Monte Carlo for Bhabha scattering at wide angles for LEP1/SLC and LEP2,” *Phys. Lett. B390*, 298-308, 1997. URL: <http://arxiv.org/pdf/hep-ph/9608412>.
- [11] “MOKKA - a detailed GEANT4 detector simulation for the Future Linear Collider.” URL: <http://polywww.in2p3.fr/geant4/tesla/www/mokka/mokka.html>.
- [12] J. Allison *et al.*, “GEANT4 developments and applications,” *IEEE Transactions on Nuclear Science 53*, No. 1, 270-278, 2006.
- [13] The FCAL collaboration - List of members can be found at: <http://www-zeuthen.desy.de/ILC/fcal/>.

- [14] H. Abramowicz *et al.*, “A Clustering Algorithm for the Luminosity Calorimeter,” *LC-PHSM-2008-006*, 2008. URL: <http://www-flc.desy.de/lcnotes/>.